Fabrication and Electrical Characterization of a Transistor Device Configuration Based on Graphene Oxide Films

D. S. Marin
University of Quindío
H. Franco-Osorio
University of Quindío
J. J Prías-Barragán (jjprias@uniquindio.edu.co)
University of Quindío

Article

Keywords:

Posted Date: July 10th, 2023

DOI: https://doi.org/10.21203/rs.3.rs-3126123/v1

Additional Declarations: No competing interests reported.

Fabrication and Electrical Characterization of a Transistor Device Configuration Based on Graphene Oxide Films

D. S. Marin[1,2,+], H. Franco-Osorio[1,2,+], and J.J Prías-Barragán[2,3,*,+]

[1]Electronic Engineering Program, Universidad del Quindío, Quindío, Armenia, 630004, Colombia
[2]Interdisciplinary Institute of Sciences,Universidad del Quindío, Quindío, Armenia, 630004, Colombia
[3]Doctoral program in Physical Sciences and Electronic Instrumentation Technology program,Universidad del Quindío, Quindío, Armenia, 630004, Colombia
[*]jjprias@uniquindio.edu.co
[+]these authors contributed equally to this work

ABSTRACT

The films of graphene oxide multilayer synthesized from bamboo as material source (GO), by the method of double thermal decomposition (DTD-method), for carbonization temperatures of 973 and 1023 K, exhibited electrical behavior as semiconductor with narrow band-gap energy and conduction mechanism by the Mott 3D variable range hopping, postulating this material as an excellent candidate for the development of electronic devices. This work presents the fabrication procedure and electrical characterization of a transistor configuration based on GO films (GOT). The electrical characterization was carried out in an automated system at low power and it were measured the transistor curves families of input, output, reaction and transfer in GOT devices. The results obtained suggest that GOT devices could be used in switching and voltage attenuation applications in low electrical power circuits, given the electrical behavior obtained as voltage dependent voltage sources with unitary gain approximately.

Introduction

In the field of electronics, graphene has been found to have a promising future, to the point of considering that its discovery contributed to the beginning of a post-silicon era, since from the work of A. Geim and K. Novoselov[1,2] opened the way for research to elucidate the interesting electrical and thermal properties of this material[3–9], giving way to the development of advanced electronics of sensor and devices.

Given this scenario J. J. Prías-Barragán and co-workers have proposed a new method for the synthesis of GO films from wastes products of the bamboo industry, so called the Double Thermal Decomposition (DTD) method, with efficient and effective process characteristics (efficiency estimate of 88 % and process times at 30 hours), low implementation cost and environmentally sustainability. The results obtained from the studies of the physical properties in GO films, suggest potential applications in the field of advanced electronics of sensor and devices, due to that it's a material with polycrystalline structure, 5.3 % of oxides concentration, vibrational behavior of a thermal insulating material, an electrical semiconductor response of narrow band gap energy (0.11 – 0.30 eV) and a magnetic behavior of ferromagnetism order at room temperature, induced by hydroxyl bridges in GO[10,11].

Globally, research has been developed using graphene and/or graphite as material for the study and development of transistor devices, among which are the design and simulation of a bipolar junction transistor (BJT) based on graphene[12]; a theoretical approach to graphene-based vertical heterojunction transistors[13], a graphene-based heterojunction transistor[14]; Field effect transistors (FET) employing GO obtained from aqueous honey solutions as raw material[15], thin film transistors (TFT) based on graphene thin films on a flexible latex substrate using a low temperature printing method[16,17] and TFTs made from GO[18,19], among others. In addition, the use of graphene in the development of various electronic and opto-electronic devices has been reported[20–28].

This demonstrated that the achievement of the development of GO-based transistors constitutes an open field of research and a great opportunity for technology development. Therefore, in this work were presented the development of a new GO-based transistor configuration, which was realized under a new proposed electrode configuration; also, the fabrication, electrical characterization, identification of hybrid parameters and discussion of possible applications of the proposed devices, are presented in this work.

Materials and Methods

Sample preparation

The synthesis of GO films was obtained by means of the Double Thermal Decomposition (DTD) method of the precursor bamboo (Guadua angustafolia Kunth), as source material, implemented in the organic materials laboratory at Universidad del Quindío, Colombia, since it is an efficient, low-cost and environmentally sustainable method[11,29,30].

This method consists of 3 stages, in the first stage bamboo slats were obtained, it was subjected to a mechanical cleaning and cutting processes. In the second stage, pyrolytic acids were obtained from bamboo, this was achieved by introducing the bamboo slats in a pyrolysis system with a controlled low nitrogen atmosphere, which allowed carbonization of the bamboo slats at different temperatures. Finally, quartz substrates covered by GO films were obtained, this was carried out starting from quartz substrates previously cleaned by means of an ultrasound bath in isopropanol, these quartzes were covered by a thin layer of pyrolytic acids obtained in the previous stage, this was achieved using the roll-coating method, to later be subjected to a second carbonization processes similar to the one carried out in the previous stage[11,29,30]. In this work, GO films synthesized at different carbonization temperatures were obtained at 973 K for GOT-37 and 1023 K for GOT-55 and GOT-83.

The authors confirm that the research methodology used on plants, such as the commercial waste of Bamboo-Guadua angustafolia Kunth, it was carried out in accordance with the relevant regulations.

Device configuration

The proposed GOT device consists of a GO-film electrically contacted employing ultra-pure silver thick film, as presented in Figure 1(a), where the GO film is deposited on an adhesive substrate, and four metallic terminals are placed on top of the film, as emitter, collector and base terminals.

In this configuration the GO-film exhibited p-type material behavior (established by hot probe method), due to its semiconductor electrical response, attributed to the presence of hydroxyl bridges, as previously reported[10].

The terminals were elaborated employing a silver (Ag) thin film deposited by cathodic erosion, due to the high electrical conductivity of this material, which provided free electrons at the metal-semiconductor junction, obtaining a similar structure present in conventional BJT transistors, as presented in Figure 1(b). Figure 1(c) shows the devices configuration proposed here. It is possible to observe that device configuration is given by Bakelite/adhesive substrate/GO-film/ultra-pure silver thick film/Cu electrical contact. The Cu electrical contact were used to interconnect silver thick film with terminals so called here as collector (C), base (B) and emitter (E) and presented in Figure 1(c).

Device manufacturing

The GO-films/quartz were deposited on a watch glass with isopropanol up to the edge, and with the help of a scalpel the films were mechanically transferred to an acrylic support where thin cuts were made on the films, reaching lateral dimensions of $1.5 \times 1.5mm$ and thicknesses of $5m$; then, the GO films were deposited on an adhesive substrate, adhered to the printed electric bakelite circuit with electrical contacts and evaporation of Ag atoms in a vacuum hood by forming a thick film. The deposition of electrical contacts of the Ag connection terminal type was achieved, with thicknesses of $200nm$.

In Figure 2, digital photographs of the GOT devices proposed and elaborated here are shown. The surfaces between straight paths (delimited by the blue lines) correspond to the surfaces of the GO-films without metal contacts; these surfaces are responsible for the input and output impedances of the GOT devices.

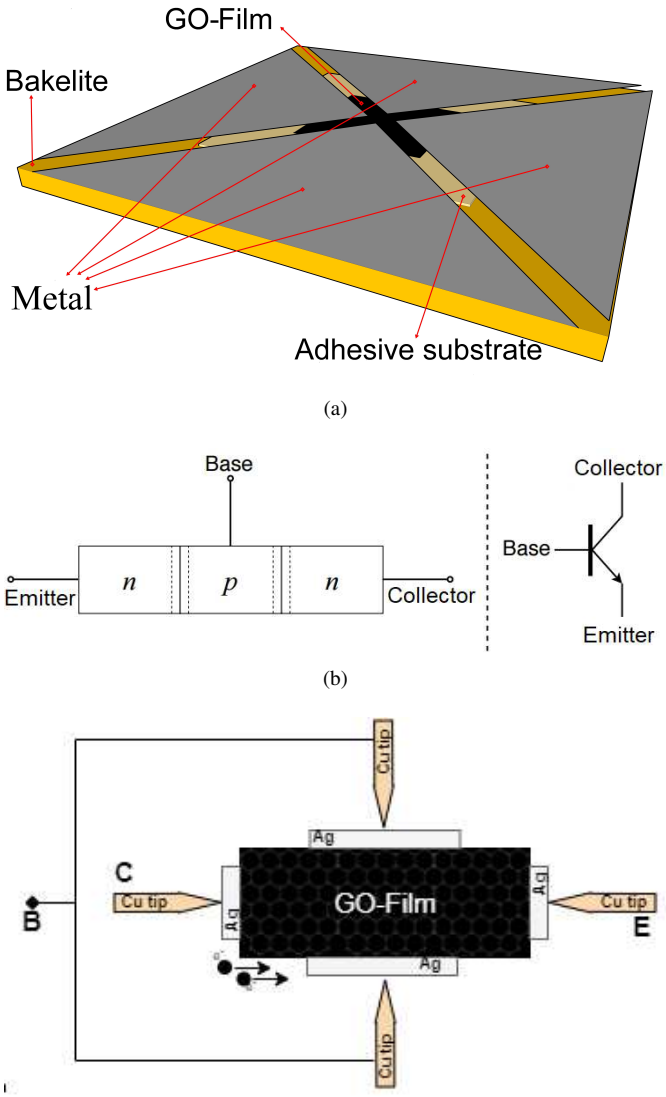

Figure 1. (a) 3D schematic representation of GOT. (b) Device structure Conventional NPN transistor device.31,32 (c) Device structure of GOT.

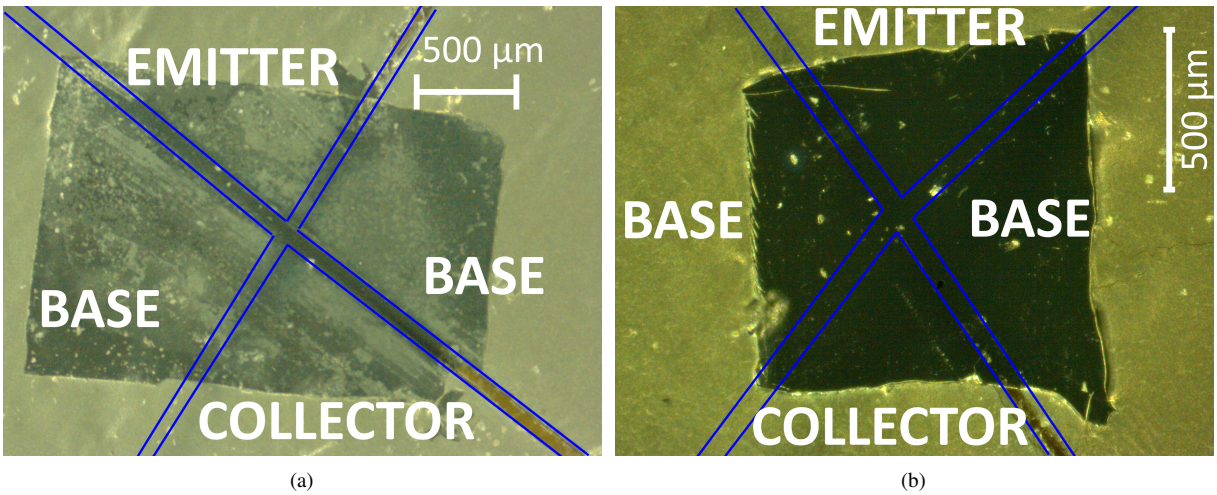

Figure 2. Photographs of two GO films with blue marked area corresponding to the absence of silver electrical contact in devices: (a) GOT-55 and (b) GOT-83. Taken using Carl Zeiss Discovery V8 stereoscope.

Characterization methods

Structural and vibrational properties of GO samples

For the structural characterization of the GO films, the X-ray diffraction technique was used, where the diffraction patterns were obtained using a Panalytical systems diffractometer, employing CuKa radiation ($\alpha = 1.542$Å). For the vibrational study, Raman spectra were obtained in a range of 500 to 4000 cm^{-1} at room temperature, using a Horiba Jobin Yvon confocal equipment, model Labram HR, working at a wavelength of 632.8 nm with a power of 0.25 mW.

Electrical characterization method

The electrical characterization of the GOT devices was carried out from the four curves families of transistor characteristics, which are input, output, reaction and transfer curves; where the measurement of currents and voltages is required, both at the input and output of the transistor devices. This was carried out using the circuit configuration shown in Figure 3. It can be seen that this is a common-emitter configuration, in which base current $\mathbf{I_B}$, collector $\mathbf{I_C}$ and emitter $\mathbf{I_E}$, base-emitter voltage $\mathbf{V_{BE}}$ and collector-emitter voltage $\mathbf{V_{CE}}$ are measured.

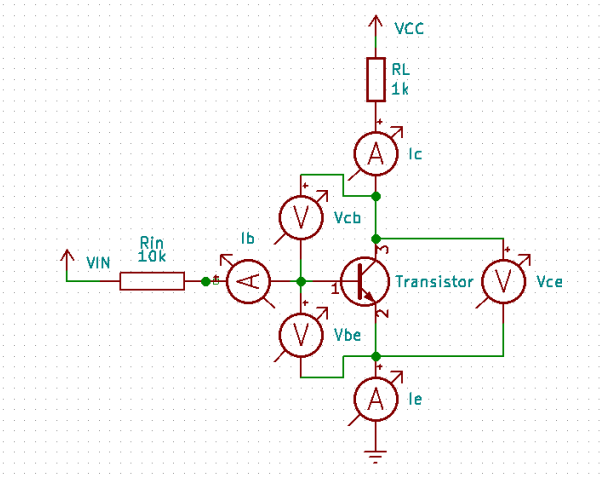

Figure 3. Assembly of the transistor device in common emitter configuration, used in this work to determine the hybrid parameters of transistor measure here.

In the results analysis of the electrical characterization of transistors here, the quadrupole model of Figure 4 was used, which considers the transistor as a two-port network, employing four variables (two voltage and two current variables, both at the input and output of a black box), it was possible to model the electrical behavior of the proposed transistor devices.

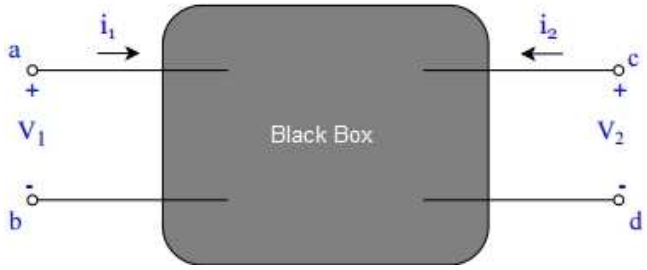

Figure 4. Two-port network, black box model. Taken and adapted from references[31–33].

From the quadrupole model, it was possible to obtain the hybrid parameters of the GOT devices, establishing two variables as independent variables and the remaining as dependent variables. For the case of the hybrid model used in this work, equations (1) and (2) were used[31–34], allowing the determination of the hybrid parameters h_{11}, h_{12}, h_{21} y h_{22} and given by:

$$\mathbf{V_{BE}} = h_{11}\mathbf{I_B} + h_{21}\mathbf{V_{CE}}, \tag{1}$$

$$\mathbf{I_C} = h_{21}\mathbf{I_B} + h_{22}\mathbf{V_{CE}}, \tag{2}$$

Where h_{11} corresponds to the input impedance, h_{12} is the reverse voltage gain, h_{21} collector current amplification factor, and h_{22} is the output impedance.

Results and discussion

Structural and vibrational results

The structural and vibrational characteristics of graphene oxide (GO) samples synthesized at 773 K are reported in this study. Structural characterization was conducted using the DRX technique, which revealed diffraction peaks at 26.58° (002), 43.34° (100), 44.48° (101), and 54.43° (004) (Figure 5(a)), indicating crystal broadening as expected for graphite-based materials. Vibrational characterization was performed by Raman spectroscopy, with the resulting data shown in Figure 5(b). The G band peak appeared at approximately 1600 cm^{-1}, and the D band at around 1330 cm^{-1}, indicating the presence of sp2 carbon bonds and structural defects such as vacancies or impurities, commonly found in disordered or amorphous carbonaceous materials. In addition, an extra band at around 2800 cm^{-1} was observed, indicating the presence of graphene multilayers with structural defects and an altered atomic structure compared to typical sp3 carbon bonds. Additionally, the HR-TEM micrograph of the films used in this study is presented, which shows the structure of a disordered material, as depicted in Figure 5(c).

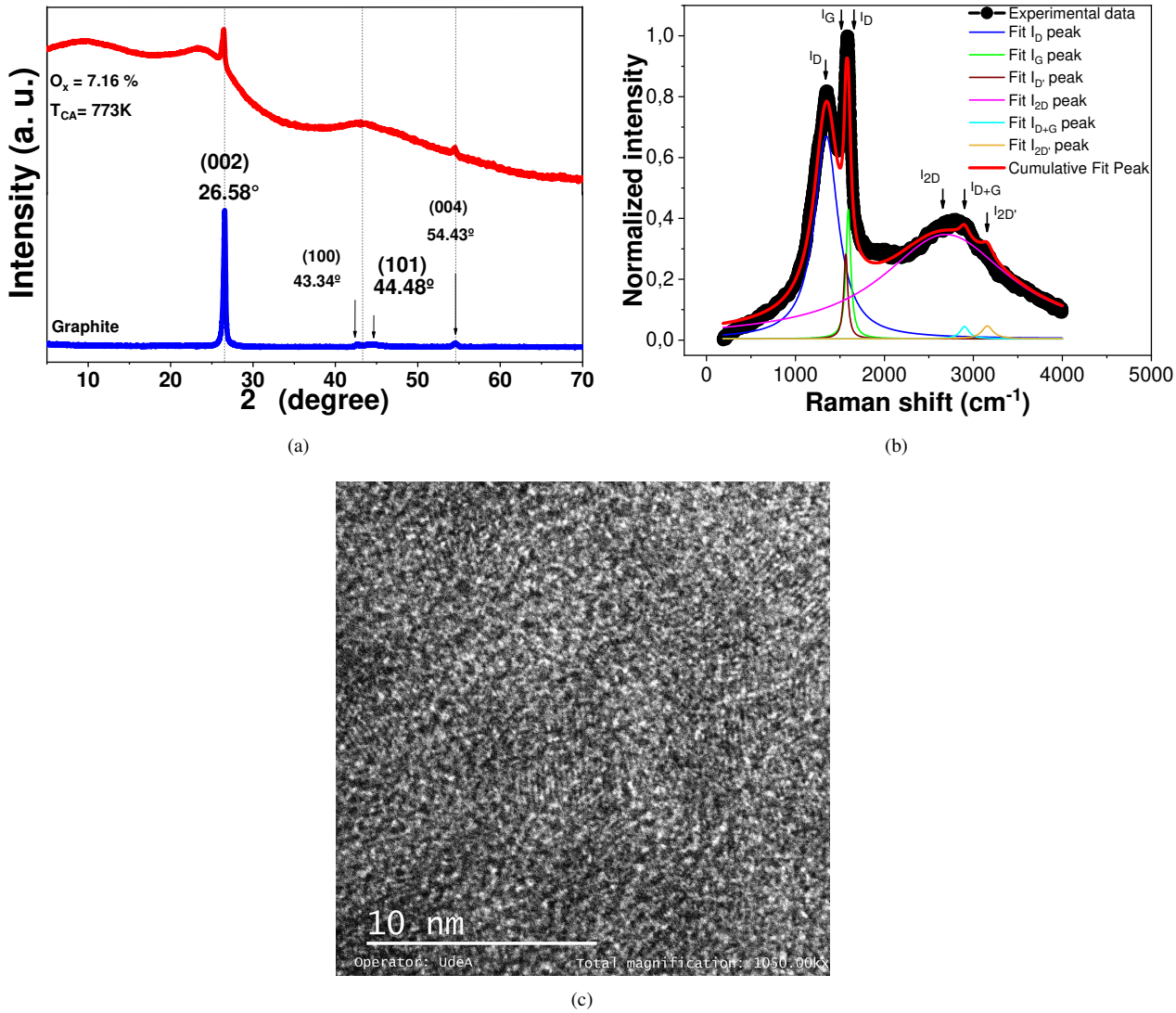

Figure 5. Structural and vibrational characterization of GO samples syntesized at 773 K. (a) DRX and (b) RAMAN y (c) TEM.

Electrical response

The measurements performed on the GOT-37, GOT-55, GOT-83 and 2N2222A (as commercial reference) devices, were carried out at room temperature, humidity and pressure, in an automated electronic system for the electrical characterization of transistors, proposed here.

Input curves

The input curves relate the dependence between input current and input voltage; that is, $\mathbf{I_B} = f(\mathbf{V_{BE}})$, for a constant V_{CC}; from this relationship the parameter h_{11} (Input Impedance) can be obtained, which is defined as the factor between $\mathbf{V_{BE}}$ and $\mathbf{I_B}$.

Figure 6 presents the family of input curves in GOT devices and 2N2222 device, for different polarization voltages V_{CC}; finding that as V_{CC} increases, the threshold voltage increases systematically, which could be attributed to the presence of Early effect, as expected. Also, it can be observed that in the GOT devices, the base currents ($\mathbf{I_B}$) presented positive and negative values, different to response that it was found in the 2N2222 device; which could possibly be associated to the ambipolar behavior of the GO films. In Figure 6(a) a nonlinear behavior can be observed with threshold voltages from 1.5 to 2.4V, due to metal-semiconductor junction effects, which agrees with the nonlinear behavior observed experimentally in the 2N2222 reference device; while in Figure 6(b) and 6(c) an ohmic type electrical response was observed, evidencing the loss of the metal-semiconductor junction effect; possibly influenced by the TCA in the fabrication of GO and the spacing between electrodes.

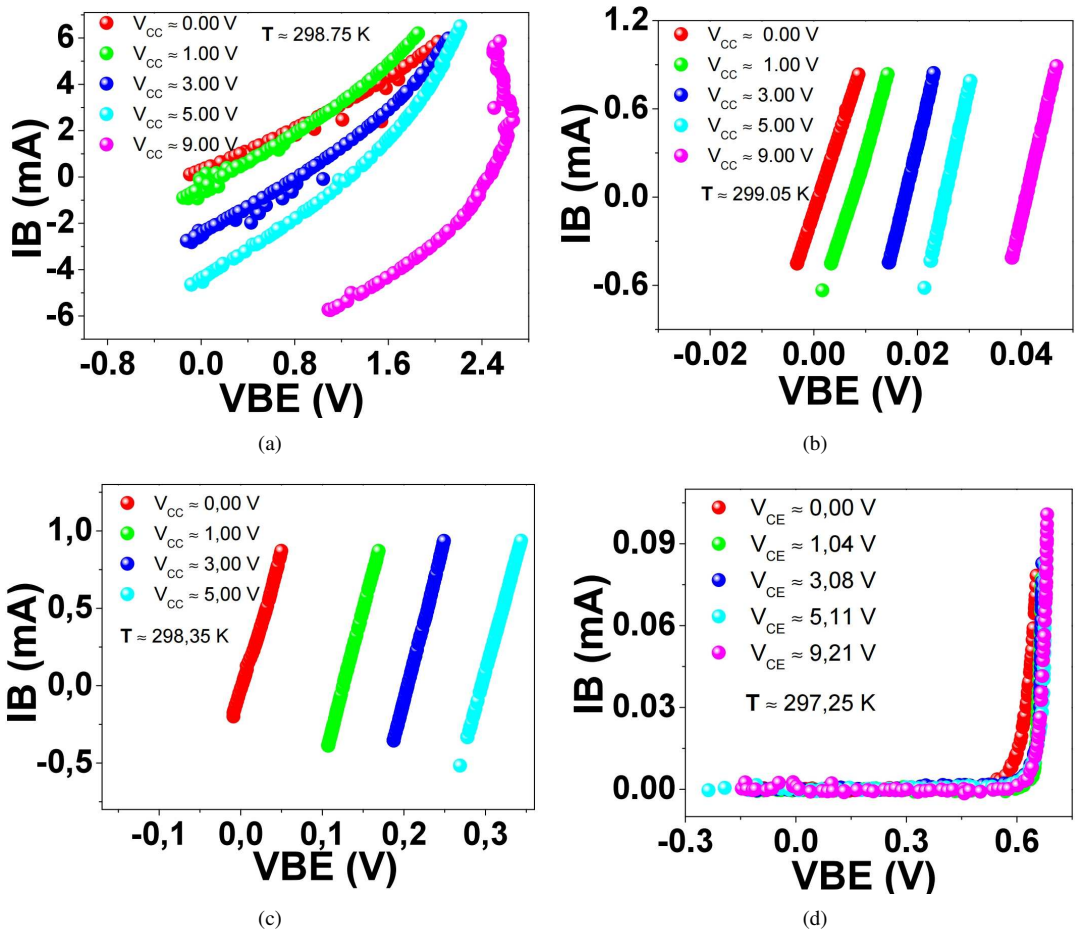

Figure 6. Family of input curves in different devices. (a) GOT-37 (TAC = 973K and 75 µm electrical contact spacing), (b) GOT-55 (TAC = 1023K and 63 µm electrical contact spacing), (c) GOT-83 (TAC = 1023K and 63 µm electrical contact spacing) and (d) Commercial transistor, reference 2N2222A.

The curves where $V_{CC} \approx 0.00V$, correspond to curves with semiconductor diode type behaviors, at the base-emitter junction and the fitting of the experimental data was performed, using the Shockley model of the semiconductor diode, described by

equation (3)[33], as presented in Figure 7.

$$\mathbf{I_B} = I_S e^{(qV_{BE})/(\eta kT)} - 1. \tag{3}$$

Here $\boldsymbol{T}$ corresponds to the measurement temperature in Kelvin, $\boldsymbol{q}$ is the electron charge, $\boldsymbol{k}$ is the Boltzmann constant, $\mathbf{I_S}$ is the inverse saturation current and η is called the diode ideality factor.

From the respective analysis of the results in Figure 7, the saturation currents and ideality factors for the different devices were found, as can be seen in Table 1, these parameters present high values compared to the values determined in the 2N2222A transistor, which could be attributed to the ambipolar characteristic of the GO samples and the effects of the low input impedances exhibited by the GOT devices.

The insets in Figure 7 show the influence of the base-emitter voltage on the input conductance, varying from 2.77 to 10.24S. These values are higher than those determined in the 2N2222A transistor, possibly due to the high mobility exhibited by the GO films[29,35].

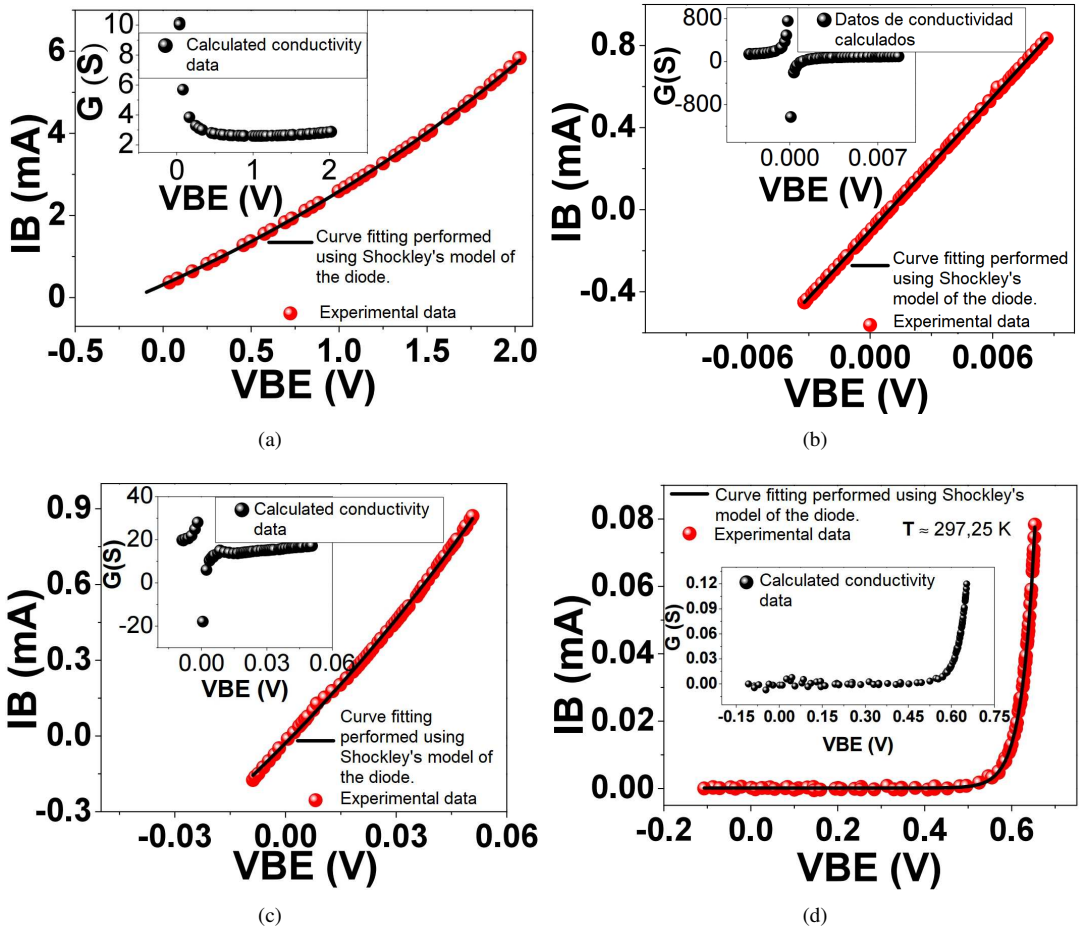

Figure 7. Input curves in different devices for a $V_{CC} \approx 0.00V$, described by the Shockley model (Continuous curve in black color). Inset, influence of the base-emitter voltage on the input conductance, in the devices: (a) GOT-37, (b) GOT-55, (c) GOT-83 and (d) 2N2222A.

In the calculation of the parameter h_{11}, the input curves of Figure 6 taken at a fixed polarization voltage of $V_{CC} \approx 5.00V$ were selected, which were adjusted employing a linear expression, since this parameter is defined as the inverse of the slope on the straight line, these calculated values are in Table 1. It can be seen that the GOT-37 device, presented an input impedance that matches the order of magnitude of the silicon-based transistor 2N2222A.

Output curves

The output curves can be obtained as the influence of output voltage in the output current or $\mathbf{I_C} = f(\mathbf{V_{CE}})$, for a fixed V_{IN}, which causes $\mathbf{I_B}$ as a fixed parameter, thus obtaining the parameter h_{22} (output admittance), this admittance is defined as the factor between $\mathbf{I_C}$ and $\mathbf{V_{CE}}$.

Figure 8 shows that $\mathbf{I_C}$ increases proportionally with $\mathbf{V_{CE}}$, this proportionality is linear in the GOT-55 and GOT-83 devices and nonlinear in the GOT-37 device. The linear dependencies were associated with ohmic contact effects, while the nonlinear ones were attributed to metal-semiconductor junction effects. In addition, it can be observed in the GOT devices, that $\mathbf{I_C}$ in the active region exhibits positive and negative values as $\mathbf{V_{CE}}$ varies, which could be attributed to the ambipolar conduction of GO, due to the presence of holes as majority carriers and electrons as minority carriers.

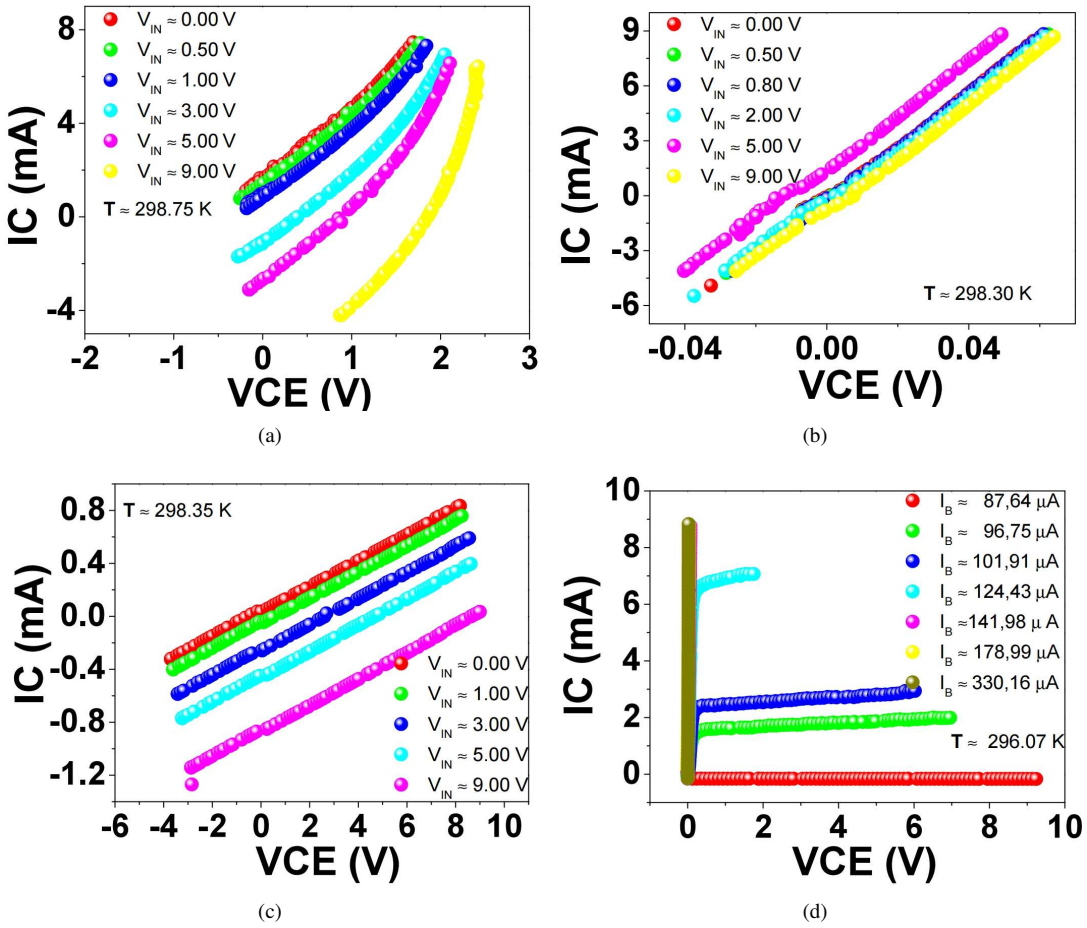

Figure 8. Family of output curves obtained in different devices. (a) GOT-37, (b) GOT-55, (c) GOT-83 and (d) 2N2222A.

In the determination of the parameter h_{22}, the curves of Figure 8 were selected for a fixed voltage of $V_{IN} \approx 5.00V$, to which a linear theoretical adjustment was made, since this parameter is defined as the slope of the straight line; from the respective analysis, the values of h_{22} presented in Table 1 were calculated. It can be seen that the GOT devices could exhibit output admittances in the range of 0.0971 to $150.1mS$, which cover the order of magnitude of 0.31 mS determined in the 2N2222A transistor in this work.

Transfer curve

The transfer curves show the variation of the output current by changes in the input current, i.e. $\mathbf{I_C} = f(\mathbf{I_B})$, for a fixed value V_{CC}, from this relationship we obtain the parameter h_{21} (collector current amplification factor) also known as β, which is defined as the factor between $\mathbf{I_C}$ and $\mathbf{I_B}$.

From Figure 9 it can be seen in the GOT devices, that an increase of voltage in V_{CC}, produces a systematic shift towards higher values of $\mathbf{I_C}$, as expected; however, it was obtained that $\mathbf{I_C}$ is inversely proportional to $\mathbf{I_B}$, this behavior that is far from what is expected in BJT transistors, as shown in the family of curves obtained for the reference device (see Figure 9(d)). In Figure 9(b) and 9(c), linear behavior and approximately zero slope are observed, this suggests independence of $\mathbf{I_C}$ with respect to $\mathbf{I_B}$.

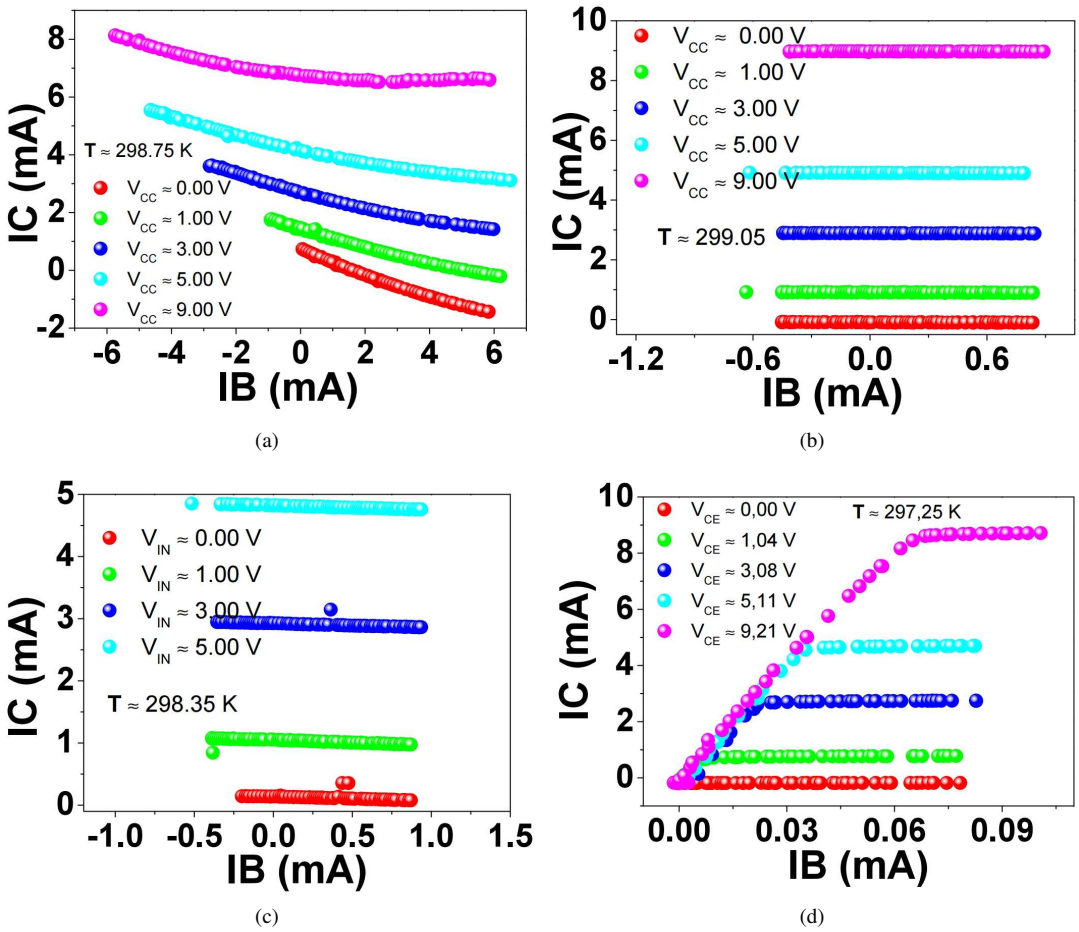

Figure 9. Family of transfer curves obtained in different devices. (a) GOT-37, (b) GOT-55, (c) GOT-83 and (d) 2N2222A.

Calculations of h_{21} parameter values were carried out by selecting curves from Figure 9 for a fixed value of $V_{CC} \approx 5V$, to which a linear theoretical fit of the experimental data was performed, with h_{21} defined as the slope of the straight line, obtained from the above fit, the calculated values are presented in Table 1. It can be observed that for the GOT devices, negative values of parameter h_{21} were obtained from 0.0136 to 0.1490 ± 0.0001, which may be associated with recombination effects of electron-hole pairs between the base and emitter terminals; which, due to their low input impedance, when $\mathbf{I_B}$ increases, the number of carriers that reach the collector terminal decreases. These low values of parameter h_{21} imply that the GOT devices, it exhibits their behavior independently of current-sources controlled by current.

Reaction curve

The reaction curves studied the effect of output voltage in the input voltage or $\mathbf{V_{BE}} = f(\mathbf{V_{CE}})$, for fixed V_{IN}; which results in $\mathbf{I_B}$ as a fixed parameter, from which the value of the parameter h_{12} (voltage inverse amplification factor), which is defined as the factor between $\mathbf{V_{BE}}$ and $\mathbf{V_{CE}}$, can be estimated.

Figure 10 shows the families of reaction curves in the characterized devices, where it is observed that in the GOT devices, the voltage $\mathbf{V_{BE}}$ increases proportionally with $\mathbf{V_{CE}}$ and independent of the voltage $\mathbf{V_{IN}}$ different behavior to that exhibited by the 2N2222A device as presented in Figure 10(d), in which an independence of $\mathbf{V_{BE}}$ with respect to $\mathbf{V_{CE}}$ can be appreciated.

In the determination of the h_{12} parameter, the reaction curves of Figure 10 were used in which $V_{IN} \approx 5V$, and from the respective linear theoretical fit, the h_{12} parameters presented in Table 1 were obtained. It can be observed that the values of parameter h_{12} in the GOT devices, ranged from 0.6140 to 0.9904 ± 0.0001, being much higher than the value obtained in the 2N2222A transistor (-0.0035), this result suggests that the GOT devices, exhibit a transistor behavior dominated by a voltage source-controlled by voltage.

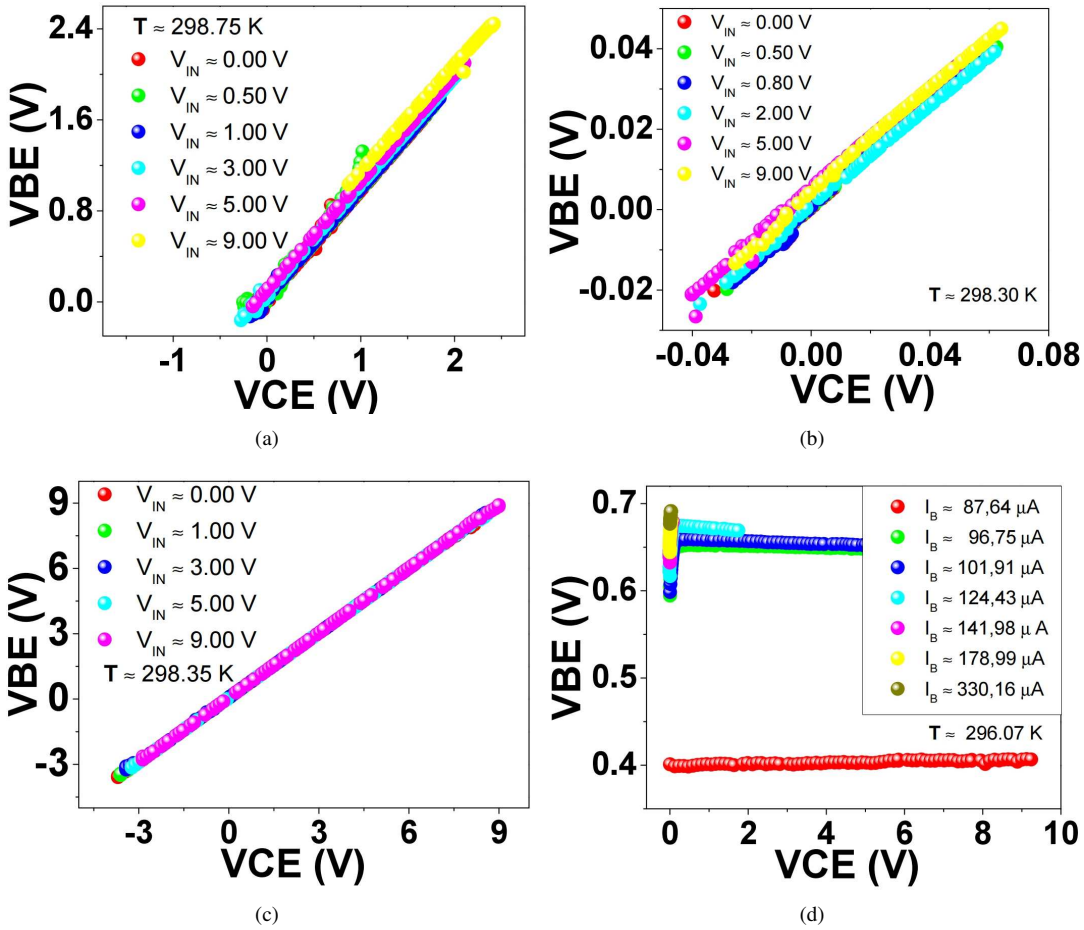

Figure 10. Family of reaction curves in different devices. (a) GOT-37, (b) GOT-55, (c) GOT-83 and (d) 2N2222A.

Proposed equivalent circuit

From the experimental results, an equivalent circuit model was proposed here, due to the parameters obtained from h_{11}, h_{12}, h_{21} and h_{22} as shown in Table 1, which were obtained following the black box modeling of transistors via the hybrid parameter quadrupole model (H).

Table 1. Parameters of the Shockley model and hybrid parameters, obtained.

Parameters	GOT-37	GOT-55	GOT-83	2N2222A
I_S	$6.3 \pm 0,1$	220 ± 187	2.3 ± 0.2	$3.0E-11 \pm 0,3E-11$
η	126 ± 2	79 ± 67	$6,1 \pm 0,4$	$1,18 \pm 0,01$
$h_{11}(\Omega)$	$123,46 \pm 0,002$	$6,219 \pm 0,001$	$51,733 \pm 0,001$	$294,12 \pm 0,08$
h_{12}	$0,9479 \pm 0,0006$	$0,614 \pm 0,001$	$0,9904 \pm 0,0005$	$-0,0035 \pm 0,0001$
h_{21}	$-0,149 \pm 0,003$	-0.0136 ± 0.0002	-0.0689 ± 0.006	141 ± 1
h_{22} (mS)	$6,9 \pm 0,01$	$150,1 \pm 0,6$	$0,09713 \pm 0,0002$	$0,31 \pm 0,02$

This is how the equivalent circuit model for the GOT devices, has presented in Figure 11, it can be seen that the parameter h_{11} corresponds to an input impedance connected in series with a voltage source controlled by voltage ($h_{12}V_2$). A current source controlled by current ($h_{21}i_1$) with a high attenuation effect of the electric fuzzy logic current, connected in parallel with the output impedance ($1/h_{22}$), can be seen at the output. Due to the high value exhibited by parameter h_{12}, compared to h_{21}, it can be established that the GOT devices presented in this work, base their transistor behavior on a voltage source controlled by voltage.

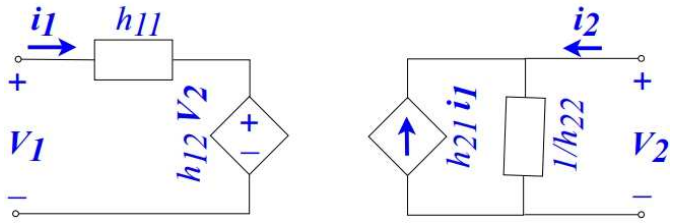

Figure 11. Equivalent circuit of the proposed GOT devices.

Potential applications

Considering a possible voltage source controlled by voltage transistor behavior on the GOT devices proposed in this work, some of their potential applications are proposed below. *(1)* Low input impedance circuits for telecommunications. The low input impedance exhibited by the GOT devices (h_{11} in Table 1), suggests that it is possible to obtain input impedance values of the order of 50Ω, as required in the input stage of electronic circuits required in telecommunications. *(2)* Switching circuits for fuzzy or tristate logic. The GOT devices exhibited collector currents with positive and negative values as the collector-emitter voltage varied here (see Figure 8). This is experimental evidence that it is possible to develop switching or voltage attenuator circuits with tri-state logic using the proposed GOT devices. *(3)* High switching efficiency circuits. The low output impedance exhibited by GOT devices ($1/h_{22}$) suggests that the switching efficiency of the GOT device in a switch circuit application can be higher than that exhibited by BJT devices. This is of great interest in the field of advanced switching circuits. *(4)* Voltage attenuator circuits, oscillators, active filters, integrators and derivers the voltage source controlled by voltage; behavior found in GOT devices suggests typical applications such as those known in unity-gain operational amplifiers.

Conclusion

The research carried out allowed first experiments in the elaboration and electrical characterization of a transistor configuration based on GO synthesized by the DTD method; in these devices, Shockley-type metal-semiconductor junction effects, NPN-type transistor behaviors, presence of Early effect and voltage source controlled by voltage, electrical behavior were identified. We propose black-box methodology for the study of GOT devices. The results suggest potential applications of GOT devices in some electronic circuits.

References

1. Geim, A. K. & Novoselov, K. S. The rise of graphene. *Nat. Mater.* **6**, 183–191, DOI: 10.1038/nmat1849 (2007).
2. Novoselov, K. S. *et al.* Two-dimensional gas of massless dirac fermions in graphene. *Nature* **438**, 197–200, DOI: 10.1038/nature04233 (2005).
3. Zhu, J., Yang, D., Yin, Z., Yan, Q. & Zhang, H. Graphene and graphene-based materials for energy storage applications. *Small* **10**, 3480–3498 (2014).
4. Yung, K. C., Wu, W. M., Pierpoint, M. P. & Kusmartsev, F. V. Introduction to graphene electronics - a new era of digital transistors and devices. *Contemp. Phys.* **54**, 233–251, DOI: 10.1080/00107514.2013.833701 (2013).
5. Singh, V. *et al.* Graphene based materials: past, present and future. *Prog. materials science* **56**, 1178–1271 (2011).
6. Zhu, Y. *et al.* Graphene and graphene oxide: synthesis, properties, and applications. *Adv. Mater.* **22**, 3906–3924, (2010).
7. Balandin, A. A. *et al.* Superior thermal conductivity of single-layer graphene. *Nano letter* **8**, 902–907 (2008).
8. González, C. R. & Kharissova, O. V. Propiedades y aplicaciones del grafeno. *Ingenierıas* **11**, 17–23 (2008).
9. Neto, A. H. C., Guinea, F., Peres, N. M. R., Novoselov, K. S. & Geim, A. K. The electronic properties of graphene. **81**, DOI: 10.1103/RevModPhys.81.109 (2007).
10. Prías-Barragán, J. J. *et al.* Magnetism in graphene oxide nanoplatelets: The role of hydroxyl and epoxy bridges. *J. Magn. Magn. Mater.* **541**, 168506 (2022).
11. Prías-Barragán, J. J. *et al.* Graphene oxide thin films: Synthesis and optical characterization. *ChemistrySelect* **5**, 11737–11744 (2020).
12. Rajabi, M., Amirmazlaghani, M. & Raissi, F. Graphene-based bipolar junction transistor. *ECS J. Solid State Sci. Technol.* **10**, 111004, DOI: 10.1149/2162-8777/ac3551 (2021).

13. Liu, C., Ma, W., Chen, M., Ren, W. & Sun, D. A vertical silicon-graphene-germanium transistor. *Nat. communications* **10**, 1–7 (2019).

14. Strobel, C. *et al.* Demonstration of a graphene-base heterojunction transistor with saturated output current. *J. Appl. Phys.* **125**, 234501 (2019).

15. Reddy, V. *et al.* Scalable production of water-dispersible reduced graphene oxide and its integration in a field effect transistor. *J. Ind. Eng. Chem.* **63**, 19–26, DOI: 10.1016/j.jiec.2018.01.033 (2018).

16. Lee, S.-K. *et al.* All graphene-based thin film transistors on flexible plastic substrates. *Nano Lett.* **12**, 3472–3476, DOI: 10.1021/nl300948c (2012).

17. ki Lee, S. *et al.* Stretchable graphene transistors with printed dielectrics and gate electrodes stretchable graphene transistors with printed dielectrics and gate electrodes. 4642–4646, DOI: 10.1021/nl202134z (2011).

18. Jilani, S. M., Gamot, T. D. & Banerji, P. Thin-film transistors with a graphene oxide nanocomposite channel. *Langmuir* **28**, 16485–16489, DOI: 10.1021/la303554z (2012).

19. He, Q. *et al.* Transparent, flexible, all-reduced graphene oxide thin film transistors. *ACS Nano* **5**, 5038–5044, DOI: 10.1021/nn201118c (2011).

20. Sánchez-Trujillo, D., Osorio-Maldonado, L. & Prías-Barragán, J. Temperature dependence of electrical conductivity and variable hopping range mechanism on graphene oxide films. *Sci. Reports* **13**, 4810 (2023).

21. Wang, B. *et al.* Graphene-based composites for electrochemical energy storage. *Energy storage materials* **24**, 22–51 (2020).

22. Kobayashi, S., Anno, Y., Takei, K., Arie, T. & Akita, S. Photoresponse of graphene field-effect-transistor with n-type si depletion layer gate. *Sci. reports* **8**, 1–9 (2018).

23. He, L.-X. & Tjong, S.-C. Zener tunneling in conductive graphite/epoxy composites: Dielectric breakdown aspects. *Express Polym. Lett.* **7** (2013).

24. Choi, H.-J. *et al.* Graphene for energy conversion and storage in fuel cells and supercapacitors. *Nano Energy* **1**, 534–551 (2012).

25. Liu, Y., Yu, D., Zeng, C., Miao, Z. & Dai, L. Biocompatible graphene oxide-based glucose biosensors. *Langmuir* **26**, 6158–6160, DOI: 10.1021/la100886x (2010).

26. Liu, J., Xue, Y., Zhang, M. & Dai, L. Graphene-based materials for energy applications. *MRS bulletin* **37**, 1265–1272 (2012).

27. Llatser, I. *et al.* Graphene-based nano-patch antenna for terahertz radiation. *Photonics Nanostructures-Fundamentals Appl.* **10**, 353–358 (2012).

28. Bonaccorso, F., Sun, Z., Hasan, T. & Ferrari, A. C. Graphene photonics and optoelectronics. *Nat. photonics* **4**, 611–622 (2010).

29. Prías-Barragán, J. J., Gross, K., Ariza-Calderón, H. & Prieto, P. Graphene oxide multilayers obtained from bamboo: New synthesis method, basic properties, and future electronic applications. *Handb. Graphene, Vol. 8: Technol. Innov.* 191 (2019).

30. Prías-Barragán, J. J., Gross, K., Ariza-Calderón, H. & Prieto, P. Synthesis and vibrational response of graphite oxide platelets from bamboo for electronic applications. *physica status solidi (a)* **213**, 85–90 (2016).

31. Vass, H. *CIRCUITOS ELECTRICOS III* (2007).

32. Nilsson, J. W., Susan, R. A., Càzares, G. N. & Fernàndez, A. S. *CIRCUITOS ELÈCTRICOS* (Addison-Wesley Iberoamericana, 1995).

33. Chapa, A. C. *Electrónica II: análisis de diseño con diodos y transistores* (Universidad Autónoma Metropolitana, Unidad Azcapotzalco, División de . . . , 1996).

34. Sabah, N. H. *Electric circuits and signals* (Crc Press, 2007).

35. Gross, K. *et al.* Electrical conductivity of oxidized-graphenic nanoplatelets obtained from bamboo: effect of the oxygen content. *Nanotechnology* **27**, 365708 (2016).

Acknowledgements

This work was funded in part by Universidad del Quindío and MinCiencias project SGR BPIN: 2020000100600 internal code 1112.

Author contributions statement

Authors declare that DSM, HFO and JJP initiated the project. DSM, HFO and JJP proposed the structure of transistor device based on graphene oxide. DSM and HFO build and made the electrical characterization of this devices. Moreover, DSM and HFO conduced the calculations of hybrid parameters of the devices for describe the electrical behavior of these devices. In addition, DSM, HFO and JJP discussed the characterization results and the manuscript. Additionally, HFO wrote the manuscript with input from JJP.

Competing and financial interests

The autors declare no competing or financial interets.

Data availability statement

The data set measured, used and/or analyzed during the present study is available from the corresponding author on reasonable request.